Bilateral Symmetry of Visual Function Loss in Cone–Rod Dystrophies

Lucia Galli-Resta,[1] Benedetto Falsini,[2] Giuseppe Rossi,[3] Marco Piccardi,[2] Lucia Ziccardi,[4] Antonello Fadda,[5] Angelo Minnella,[2] Dario Marangoni,[2] Giorgio Placidi,[2] Francesca Campagna,[2] Edoardo Abed,[2] Matteo Bertelli,[6] Monia Zuntini,[6] and Giovanni Resta[7]

[1]Istituto di Neuroscienze Consiglio Nazionale delle Ricerche (CNR), Pisa, Italy
[2]Institute of Ophthalmology, Policlinico Gemelli, Catholic University, Rome, Italy
[3]Istituto di Fisiologia Clinica CNR, Pisa, Italy
[4]Bietti Foundation, Istituto di Ricovero e Cura a Carattere Scientifico (IRCCS), Rome, Italy
[5]Tecnologie e Salute, Istituto Superiore di Sanità, Rome, Italy
[6]MAGI Laboratory for Medical Genetics, Rovereto, Italy
[7]Istituto di Informatica e Telematica CNR, Pisa, Italy

Correspondence: Benedetto Falsini, Istituto di Oftalmologia, Policlinico Gemelli, Università Cattolica del Sacro Cuore, Largo Agostino Gemelli, 8, 00168, Roma; bfalsini@rm.unicatt.it.

Submitted: October 1, 2015
Accepted: June 4, 2016

Citation: Galli-Resta L, Falsini B, Rossi G, et al. Bilateral symmetry of visual function loss in cone–rod dystrophies. *Invest Ophthalmol Vis Sci*. 2016;57:3759–3768. DOI:10.1167/iovs.15-18313

Purpose. To investigate bilateral symmetry of visual impairment in cone–rod dystrophy (CRD) patients and understand the feasibility of clinical trial designs treating one eye and using the untreated eye as an internal control.

Methods. This was a retrospective study of visual function loss measures in 436 CRD patients followed at the Ophthalmology Department of the Catholic University in Rome. Clinical measures considered were best-corrected visual acuity, focal macular cone electroretinogram (fERG), and Ganzfeld cone-mediated and rod-mediated electroretinograms. Interocular agreement in each of these clinical indexes was assessed by *t*- and Wilcoxon tests for paired samples, structural (Deming) regression analysis, and intraclass correlation. Baseline and follow-up measures were analyzed. A separate analysis was performed on the subset of 61 CRD patients carrying likely disease-causing mutations in the *ABCA4* gene.

Results. Statistical tests show a very high degree of bilateral symmetry in the extent and progression of visual impairment in the fellow eyes of CRD patients.

Conclusions. These data contribute to a better understanding of CRDs and support the feasibility of clinical trial designs involving unilateral eye treatment with the use of fellow eye as internal control.

Keywords: cone dystrophy, interocular, visual acuity, visual function, electroretinography

Cone–rod dystrophies (CRDs) are a family of inherited diseases characterized by the progressive loss of the retina photoreceptors, with a primary loss of cones, typically followed by loss of rods.[1–7]

Characteristically CRDs lead to early impairment of vision, being a major cause of severe visual impairment and blindness in children and young adults.[8] There is presently no cure for CRDs, but a number of promising therapeutic strategies are under investigation at the preclinical level.[9–11]

In the great majority of cases CRDs affect both eyes, and it is the general clinical impression that the loss of visual function is symmetrical in the two eyes of CRD patients.[12,13] This view is supported by quantitative studies, reporting bilateral symmetry in fundus appearance,[14–16] visual acuity,[14] and multifocal ERG recordings.[17] These studies, however, are limited to small patient cohorts.

Quantifying bilateral symmetry of visual loss in a large cohort of CRD patients may contribute to a better knowledge of these diseases and help design clinical trials, because bilateral symmetry is a necessary condition for trial designs with unilateral treatment and the use of fellow eye as a control, as is typically the case for retinal gene therapy.[18]

The present retrospective study examines bilateral symmetry in the loss of visual function in 436 typical CRD patients, analyzing best-corrected visual acuity, Ganzfeld cone-mediated electroretinogram (cone ERG), Ganzfeld rod-mediated electroretinogram (rod ERG), and focal macular electroretinogram (fERG) data. The analysis addresses the symmetry of baseline values and visual decay over time in the fellow eyes. A dedicated analysis has been performed for the subset of 61 CRD patients with likely disease-causing mutations in the *ABCA4* gene.

Using a set of complementary statistical tests to overcome individual test limitations, we found that visual impairment in CRDs displays a high degree of bilateral symmetry.

Patients and Methods

This retrospective study analyzed clinical data from CRD Caucasian patients clinically followed at the Visual Electrophysiology unit of the Università Cattolica del Sacro Cuore in Rome in the years 1999 to 2015. As a comparison, data from 40 normal control subjects are also illustrated.

Patients had a diagnosis of CRD based on history, clinical findings, and ERG abnormalities. They had sought consultation because of visual symptoms or as relatives of affected patients. After the first visit, patients were invited to adhere to the institutional schedule of at least one visit per year, with the exact scheduling established by an independent administrative office. All patients gave informed consent to participate to the study. The study adhered to the tenets of the Declaration of Helsinki and was approved by the Institutional Review Board.

Study patients met the following inclusion criteria: typical CRD with a cone–rod pattern of retinal dysfunction, as determined by International Society for Clinical Electrophysiology of Vision (ISCEV) standard Ganzfeld electroretinography,[19] dark-adapted Tübinger perimetry, and classic fundus appearance; inheritance pattern unequivocally determined by a detailed family and medical history; no or minimal ocular media opacities; absence of nystagmus; foveal fixation or preferred retinal locus for fixation within 3° of the fovea and stable throughout the follow-up; no concomitant ocular, visual, or systemic diseases.

Measures of Ocular Function and Electroretinography

A full general and ophthalmologic examination (including detailed family history, anterior segment biomicroscopy, best-corrected Snellen visual acuity, direct and indirect ophthalmoscopy, intraocular pressure measurement) was performed on each patient at baseline and on several consecutive visits. While ISCEV standards for ERG were followed for the first diagnostic visit, a modified protocol was used in all the subsequent visits, with electrode placement on the eyelids, which we found to be much better tolerated by patients, particularly young ones, than corneal electrodes.[20]

For ERG recordings, pupils were pharmacologically (1% tropicamide and 2.5% phenylephrine hydrochloride) dilated to a diameter $\geq$ 8 mm.

All ERGs were recorded while patients fixated monocularly a 0.25° central fixation mark under the constant monitoring of an external observer. Electroretinograms were recorded by means of an Ag–AgCl 0.9-cm-diameter skin electrode taped on the skin of the lower eyelid after coating the electrode surface with saline electroconductive gel. The electrodes were placed approximately 2.5 mm below the inferior lid rim, in the vertical axis passing through the corneal apex. A similar electrode on the lower eyelid of the contralateral patched eye was used as reference to minimize potential artifacts due to blink and conjugate eye movement.

In early diagnostic evaluations, ERG recordings were obtained by corneal electrodes following the ISCEV standards. Following a dark-adaptation period of 30 minutes, the Ganzfeld rod-mediated ERG was recorded in response to white 50-µs flashes of 0.01 cd·s/m^2. Responses were averaged over 20 stimulus presentations. Interstimulus interval was 2 seconds. Following a 20-minute adaptation to light, Ganzfeld cone-mediated ERG was recorded in response to white 50-µs full-field stimuli with an intensity of 2 cd·s/m^2 presented on a steady white background of 20 cd/m^2 of a Ganzfeld bowl. Responses were averaged over 40 stimulus presentations. Interstimulus interval was 1 second.

Signals were amplified (50 K), filtered (0.3–250 Hz), digitized at 2 KHz, and averaged over 40 runs with automatic artifact rejection. The baseline to peak rod b-wave amplitude was measured. The amplitudes of the a- and b-waves were measured as previously described.[20]

Macular cone-mediated fERG was recorded from the central 18° region using a flickering uniform red field superimposed on a constant equiluminant steady adapting background, as previously described.[21] Briefly, the stimulus was generated by a circular array of eight red light-emitting diodes (LEDs) (660 nm; maximum luminance: 93 cd/m^2) presented on the rear of a Ganzfeld bowl (luminance: 40 cd/m^2). A diffusing filter in front of the LED array made it appear as a circle of uniform red light. Focal ERGs were recorded in response to the 41-Hz sinusoidal 95% luminance modulation of the central red field. For each recording, fERG signals were amplified (100,000-fold), band-pass filtered (1–100 Hz; 6 dB/Oct), and averaged (12-bit resolution, 2-kHz sampling rate, 1200–1600 repetitions in six to eight blocks). Offline discrete Fourier analysis quantified the amplitude of the response first harmonic at 41 Hz.

Data Acquisition and Analysis

All measures were obtained monocularly on each eye in each patient. The usual routine testing sequence was as follows: right–left–left–right. Attributed to each eye was the average value of its two recordings.

Visual acuity and fERG data derive from visits performed between 1999 and 2015 under the same test and recording conditions. Ganzfeld cone-mediated ERG and Ganzfeld rod-mediated ERG data derive from visits performed between 2006 and 2015 under the same test and recording conditions. All ERG data analyzed in this study derive from measures performed with eyelid electrodes.

In agreement with previous studies, quantitative analyses were performed on the logarithm of the minimal angle of resolution (logMAR) for visual acuity fractions to minimize nonnormality,[22] the b-wave amplitude for Ganzfeld ERGs,[22] and the first harmonic amplitude for the macular fERG.[21]

Baseline data (i.e., the measures obtained on the first visit of the patient recorded in the database) were available for all four measures. Data documenting disease progression were available only for fERG and visual acuity.

The similarity of disease progression in the two eyes was studied comparing intraocular decays in fERG and logMAR values in the two eyes after 1 to 4 years from baseline. To this purpose, we quantified logMAR and fERG variations from baseline binning data in two time windows. These windows spanned from 1 to 2.5 years from baseline and from 2.5 to 4 years from baseline, respectively. In either time bin only one entry was considered for each patient. Whenever more than one entry was available for a patient, the entry at the time closer to the center of the time bin was selected.

Statistical Analysis

Because the study aimed at quantifying the extent to which the left and right eye of CRD patients were similarly affected by the disease, statistical analyses were performed considering both baseline values and intraocular decay values.

For each analyzed measure (basal value and decay value) we performed a battery of tests to compare the two eyes.

Specifically, we performed tests for paired data (*t*- and Wilcoxon rank tests) to assess whether the mean/median of the difference between left and right eye was significantly different from zero. The Deming regression was used for testing the agreement between left and right eye and the significance of a constant and a proportional bias. If the left and right eye values are plotted on an *x-y* graph, the slope and the intercept of a straight line fitted to the data points reveals the nature and magnitude of any bias present. If no bias is present, the estimated slope will not be significantly different from 1 and the intercept will not be significantly different from zero, and the regression line will correspond to the identity line. For computing the standard error and the nonparametric 95%

Investigative Ophthalmology & Visual Science

Investigative Ophthalmology & Visual Science

TABLE 1. Baseline Values

Baseline Values	Rod ERG, μV			Cone ERG, μV			fERG, μV			logMAR			logMAR > −0.69			fERG > 0.5 μV		
	OD	OS	OD-OS	OD	OS	OD-OS	OD	OS	OD-OS	OD	OS	OD-OS	OD	OS	OD-OS	OD	OS	OD-OS
CRD patients																		
Mean	35.43	36.48	1.047	13.54	14.19	−0.65	0.79	0.81	−0.019	−0.55	−0.53	−0.024	−0.203	−0.199	−0.0035	1.255	1.295	−0.040
Std. deviation	21.19	22.74	7.187	7.59	8.33	4.57	0.6	0.63	0.34	0.48	0.48	0.29	0.2	0.199	0.131	0.528	0.530	0.387
N		98			128			399			337			184			195	
Normal controls																		
Mean	50.55	49.28	1.269	25.70	25.76	−0.062	2.17	2.14	0.029									
Std. deviation	16.36	10.86	10.57	9.23	8.35	5.629	0.48	0.66	0.409									
N		40			40			40										
Lower 95%CI of mean			−2.113			−1.862			−0.102									
Upper 95%CI of mean			4.65			1.739			0.159									

OD, right eye; OS, left eye; OD-OS, distribution of the differences between the right and left eye value.

confidence interval of the slope and intercept, 5000 iterations of bootstrap resampling were used.[23]

For quantifying the degree of agreement between the measures obtained in the two eyes, the intraclass correlation coefficient (ICC) was also computed[24] by using a two-way mixed model with measures of absolute agreement. According to previous studies, ICC data can interpreted as follows: ICCs between 0.5 and 0.6 indicate moderate agreement; 0.7 to 0.8 indicates strong agreement; and >0.8 indicates almost perfect agreement (http://statstodo.com [in the public domain]). Alternatively, ICC < 0.4 = poor; 0.40–0.75 = good; > 0.75 = excellent.[25]

As a visual reference we also plotted the Bland-Altman graphs.

Matched-paired tests, ICC, and linear regression were performed using SPSS for Windows v. 20 (IBM Corp., Armonk, NY, USA). Deming regression was performed using MethComp package v. 1.22.2 of R v. 2.13.0 (R Foundation for Statistical Computing, Vienna, Austria). Additional controls were performed using Prism v.6.0 (GraphPad Software, Inc., La Jolla, CA, USA) and JMP v11.0.0 (SAS Institute, Cary, NC, USA). Data plotting was performed using Origin v. 8.5 (OriginLab Corporation, Northampton, MA, USA). A 2-tailed significance level was set at $\alpha = 0.05$.

RESULTS

The CRD patient cohort we studied comprised 436 individuals, 208 males and 228 females, with an average age at first visit (baseline) of 31.21 ± 18.85 years (age range, 4–83 years); age stratification at baseline, 60 patients (<10 years), 92 (11–20 years), 61 (21–30 years), 63 (31–40 years), 72 (41–50 years), 42 (51–60 years), and 33 (61–83 years). We analyzed measures from four clinical tests. These included best-corrected visual acuity values (converted to log decimal values of the logMAR) and the response amplitudes of three electroretinographic tests (Ganzfeld rod ERG, Ganzfeld cone ERG, and fERG recorded in response to the stimulation of the central macular 18°). To avoid confusion between the actual measurement values and the clinical tests from which the measure derives, the latter will be referred to as clinical indexes.

Intereye Comparison of Baseline Values

Table 1 summarizes for each clinical index the average baseline values and number of patients for whom we had bilateral data in the CRD cohort. For a comparison, electroretinographic data from 40 control subjects are also illustrated (average age, 33.6 ± 8.55 years; age range, 20–50 years).

Individual baseline values for logMAR, rod ERG, cone ERG, and fERG amplitudes in CRD patients are shown in Figures 1 to 4, respectively. For each clinical index, baseline measures are shown for all patients by plotting the left eye measurement against the corresponding right eye measurement (left graph), and the difference between left and right eye values against their average (Bland-Altman plot, right graph). Bilateral measures were available from 337 patients for logMAR, 98 patients for rod ERG, 128 patients for cone ERG, and 399 patients for fERG. Electroretinographic data for 40 normal control subjects are also shown.

The results of the statistical analyses testing bilateral symmetry in baseline measurements are briefly reported in the figures and shown in detail in Table 2.

For all four clinical indexes these results can be thus summarized: (1) The mean/median of the interocular difference is not significantly different from zero; (2) Deming regression analysis best linear fit is not significantly different

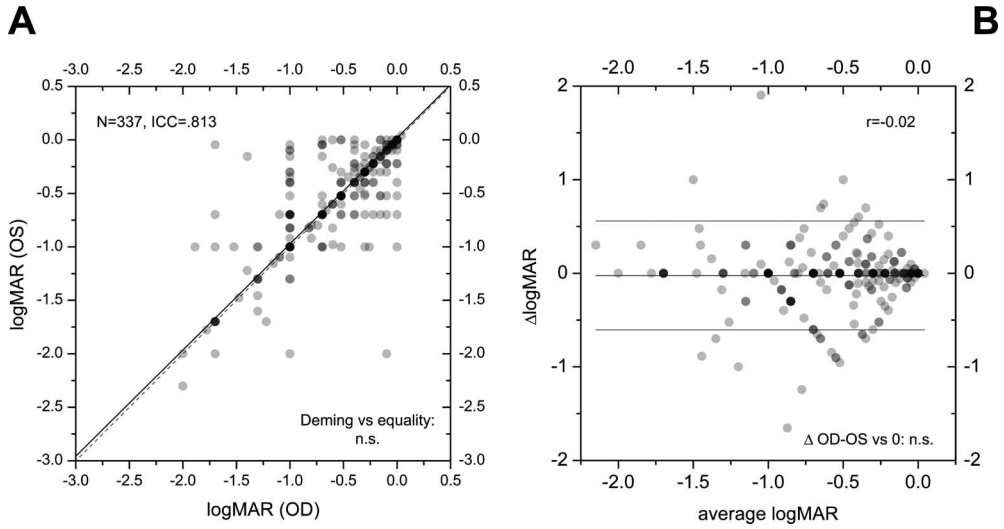

Figure 1. Bilateral symmetry in visual acuity baseline measures in CRD patients. (**A**) Baseline visual acuity for the left eye is plotted against the corresponding right eye measure for each of the 337 CRD patients with bilateral baseline acuity measures. The *continuous line* is the Deming regression line; the *dashed line* is the diagonal or equality line, where data points lie if the left and right eye measures coincide. Visual acuity is plotted as logMAR. *Dots* are partially transparent to allow the viewing of superimposed data. (**B**) The difference between right and left eye visual acuity (ΔlogMAR) is plotted against their average value (Bland-Altman plot). *Horizontal lines* indicate the mean and the mean ± 2 SD of the distribution of intereye difference in logMAR. Figure summarizes the results of statistical tests on intereye differences. Detailed results are in the Tables. OD, right eye (oculus dextrus); OS, left eye; Δ, difference; n.s., not significant; vs, versus; N, number of patients; ICC, intraclass correlation; Deming vs equality, test of Deming regression line versus equality; Δ OD-OS vs 0, test of mean/median intereye difference versus zero; *r*, Spearman correlation between difference and average intereye values; SD, standard deviation.

from the line indicating identity of the two eye measurements; and (3) the ICC has values above 0.8, indicating a very good to excellent quantitative agreement between paired measurements.[25,26]

The same results are obtained if this analysis is limited to the subset of patients in a more compact age range (20–50 years; see Supplementary Tables S1 and S2).

Taken together, these results indicate a very high degree of bilateral symmetry in baseline measurements of best-corrected visual acuity, rod ERG, cone ERG, and fERG in CRD patients.

Comparison of Disease Progression in the Fellow Eyes

We next tested whether disease progression was the same in the left and right eye of CRD patients.

This analysis comprised two parts. Firstly, we repeated the analysis of baseline measurements applying a lower threshold cutoff, to focus on patients for whom a decay in the specific clinical index would still be detectable. Secondly, we analyzed

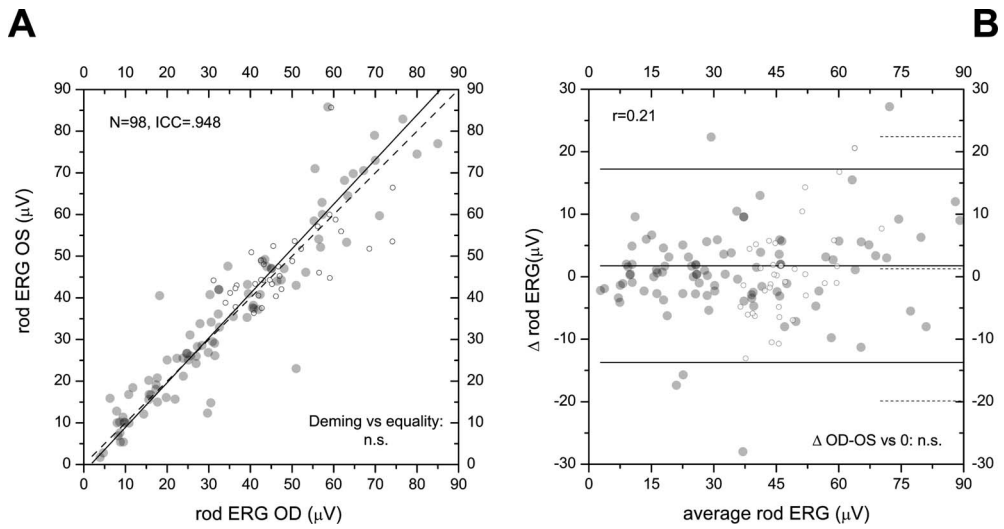

Figure 2. Bilateral symmetry in Ganzfeld rod ERG measures in CRD patients at baseline. (**A**) Baseline Ganzfeld rod ERG amplitude for the left eye plotted against the corresponding right eye measure for each of the 98 CRD patients with bilateral baseline Ganzfeld rod ERG measures (*gray dots*). *Dots* are partially transparent to allow viewing of superimposed data. The *dashed line* is the diagonal (left = right), the *continuous line* is the Deming regression line. For comparison, data from 40 normal control patients are also plotted (*open circles*). (**B**) Difference between right and left eye Ganzfeld rod ERG (Δ rod ERG) plotted against their average value (*gray dots*; Bland-Altman plot). *Horizontal lines* indicate the mean and the mean ± 2 SD of the distribution of intereye difference in Ganzfeld rod ERG amplitude. Data from 40 normal control subjects are plotted as *open circles. Dashed lines* indicate their mean and the mean ± 2 SD. Statistical summary and abbreviations as in Figure 1.

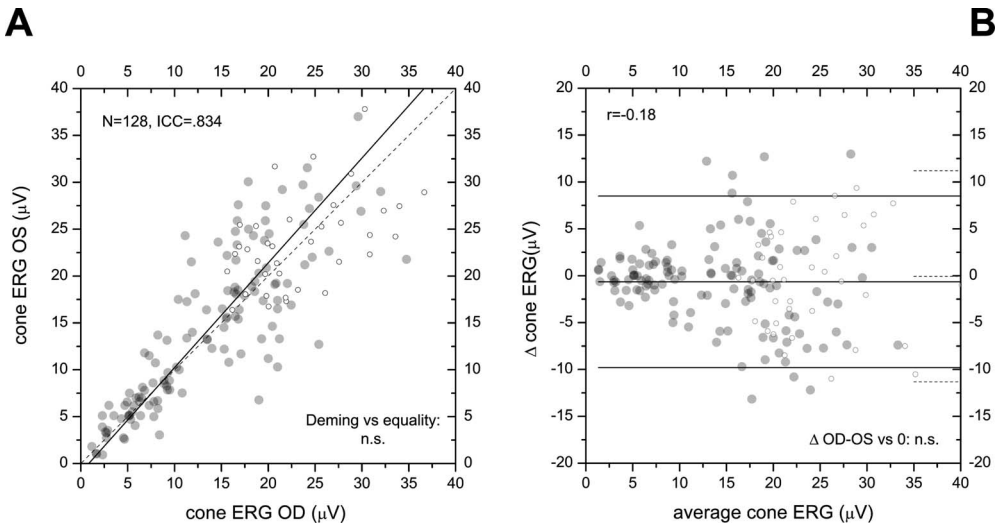

Figure 3. Bilateral symmetry in Ganzfeld cone ERG measures in CRD patients at baseline. (**A**) Baseline Ganzfeld cone ERG amplitude for the left eye plotted against the corresponding right eye measure for each of the 128 CRD patients with bilateral baseline Ganzfeld cone ERG measures (*gray dots*). *Dots* are partially transparent to allow viewing of superimposed data. The *dashed line* is the diagonal (left = right), the *continuous line* is the Deming regression line. For comparison, data from 40 normal control patients are also plotted (*open circles*). (**B**) Difference between right and left eye Ganzfeld cone ERG (Δ cone ERG) plotted against their average value (*gray dots*; Bland-Altman plot). *Horizontal lines* indicate the mean and the mean ± 2 SD of the distribution of intereye difference in Ganzfeld cone ERG amplitude. Data from 40 normal control subjects are plotted as *open circles. Dashed lines* indicate their mean and the mean ± 2 SD. Statistical summary and abbreviations as in Figure 1.

the degree of similarity of visual function decay over time between the fellow eyes.

Follow-up data were available for logMAR and fERG measurements. In agreement with previous studies we set a bottom threshold value of –0.69 for logMAR (corresponding to 2/10, the penultimate line in the Snellen chart) and 0.5 μV for fERG (a value previously identified as a cutoff to avoid floor effects in fERG time lines[21]). Bilateral measures above the set thresholds were available from 195 patients for fERG and 184 patients for logMAR (Table 1).

Figures 5 and 6 illustrate baseline data above cutoff for logMAR and fERG, respectively.

Summary statistics for intereye statistical tests are detailed in Table 3 and reported schematically in Figures 4 and 5. In summary, all tests indicated a high degree of similarity between the fellow eye baseline measurements, also in the dataset restricted to patients with measures above cutoff.

To test the degree of similarity between the fellow eyes in visual function decay over time we focused on measures obtained from 1 to 4 years from baseline, subdividing this interval in two equal bins, spanning from 1 to 2.5 years and

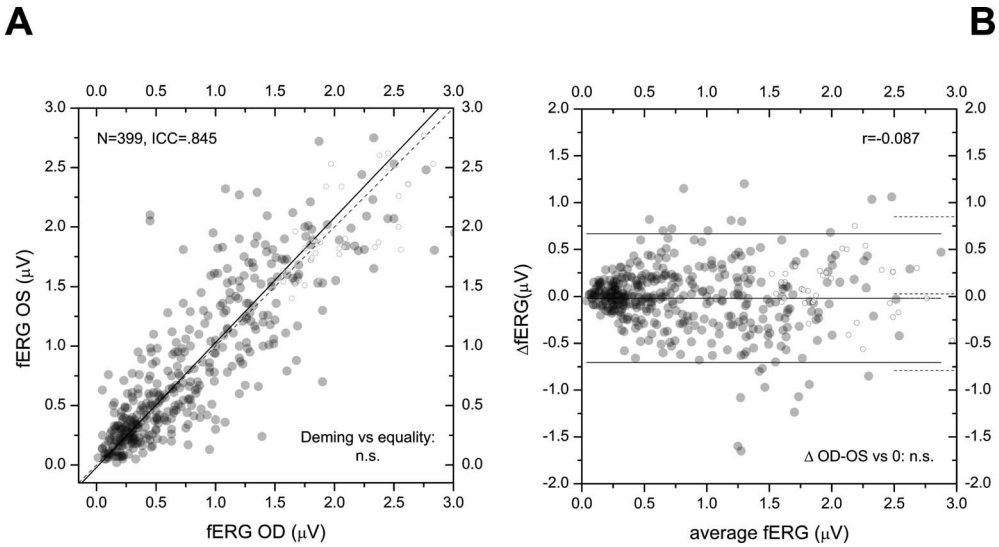

Figure 4. Bilateral symmetry in focal cone macular ERG (fERG) measures in CRD patients at baseline. (**A**) Baseline fERG value for the left eye plotted against the corresponding right eye measure for each of the 399 CRD patients with bilateral baseline fERG measures. The *dashed line* is the diagonal (left = right), the *continuous line* is the Deming regression line. *Dots* are partially transparent to allow viewing of superimposed data. For comparison, data from 40 normal control subjects are also plotted (*open circles*). (**B**) Difference between right and left eye fERG (ΔfERG) plotted against their average value (Bland-Altman plot). *Horizontal lines* indicate the mean and the mean ± 2 SD of the distribution of intereye difference in Ganzfeld cone ERG amplitude. Data from 40 normal control subjects are plotted as *open circles. Dashed lines* indicate their mean and the mean ± 2 SD. Statistical summary and abbreviations as in Figure 1.

Table 2. Baseline Statistics of Intereye Differences in Clinical Indexes for CRD Patients

	Rod ERG, μV			Cone ERG, μV			fERG, μV			logMAR			logMAR > −0.69			fERG > 0.5 μV		
Baseline	***N***	**Paired *t* Wilcoxon**		***N***	**Paired *t* Wilcoxon**		***N***	**Paired *t* Wilcoxon**		***N***	**Paired *t* Wilcoxon**		***N***	**Paired *t* Wilcoxon**		***N***	**Paired *t* Wilcoxon**	
Matched paired tests																		
Probability	98	0.1523	0.7775	128	0.109	0.098	399	0.261	0.482	337	0.132	0.17	184	0.717	0.846	195	0.155	0.164
	Estimate	**95%CI low**	**95%CI up**	**Estimate**	**95%CI low**	**95%CI up**	**Estimate**	**95%CI low**	**95%CI up**	**Estimate**	**95%CI low**	**95%CI up**	**Estimate**	**95%CI low**	**95%CI up**	**Estimate**	**95%CI low**	**95%CI up**
Deming regression																		
Intercept	−1.770	−4.650	1.116	0.939	−2.928	1.050	−0.020	−0.071	0.031	0.020	−0.016	0.055	0.003	−0.011	0.017	0.034	−0.137	0.204
Slope	1.071	1.000	1.141	1.118	0.984	1.251	1.049	0.968	1.131	0.992	0.919	1.066	0.999	0.929	1.068	1.005	0.855	1.155
ICC	0.948	0.923	0.965	0.834	0.772	0.880	0.845	0.815	0.871	0.813	0.774	0.847	0.785	0.723	0.835	0.731	0.659	0.79

CI, confidence interval of the mean; low, lower bound; up, upper bound.

Table 3. Summary of Statistical Tests of Bilateral Symmetry on logMAR and fERG Decay With Time in CRD Patients

	T1, 1–2.5 Years						T2, 2.5–4 Years					
	Delta logMAR			Delta fERG			Delta logMAR			Delta fERG		
	N	**Mean**	**SD**	***N***	**Mean**	**SD**	***N***	**Mean**	**SD**	***N***	**Mean**	**SD**
OD	48	0.1408	0.2873	64	−0.1978	0.6089	47	0.1958	0.3197	57	−0.4274	0.5053
OS		0.1275	0.2743		−0.1878	0.6058		0.1884	0.2608		−0.4397	0.5117
OD-OS		0.01302	0.1826		−0.00995	0.4845		0.007331	0.2015		0.01237	0.4091
Matched paired tests		**Paired *t***	**Wilcoxon**		**Paired *t***	**Wilcoxon**						
Probability		0.61	0.81		0.87	0.91		0.8042	0.317		0.82	0.925
	Estimate	**95%CI low**	**95%CI up**	**Estimate**	**95%CI low**	**95%CI up**	**Estimate**	**95%CI low**	**95%CI up**	**Estimate**	**95%CI low**	**95%CI up**
Deming regression												
Intercept	−0.005	−0.073	0.064	0.008	−0.163	0.180	−0.045	−0.038	0.111	0.004	−0.202	0.193
Slope	0.943	0.7255	1.616	0.992	0.722	1.263	0.801	0.58	1.024	1.019	0.719	1.319
ICC	0.789	0.652	0.876	0.682	0.525	0.794	0.764	0.623	0.858	0.676	0.510	0.796

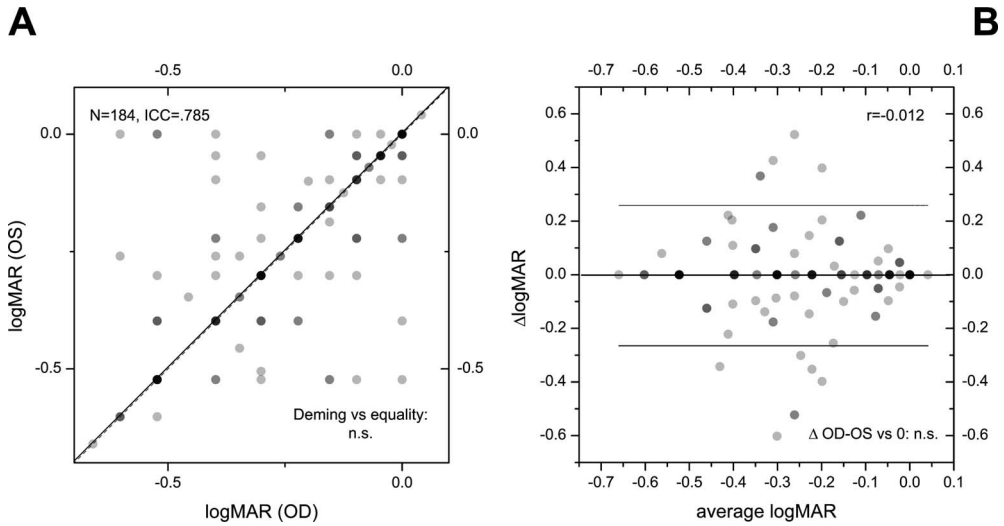

FIGURE 5. Bilateral symmetry in baseline visual acuity measures in CRD patients above cutoff. (**A**) Baseline visual acuity for the left eye plotted against the corresponding right eye measure for each of the 184 CRD patients with baseline logMAR > -0.69 (2 decimals) in both eyes. *Dashed line* is the diagonal, *continuous line* is the Deming regression line. *Symbols* are partially transparent to allow viewing of superimposed data. (**B**) Bland-Altman plot for the same data as in (**A**). The mean and mean ± 2 SD lines are indicated. Statistical summary and abbreviations as in Figure 1.

from 2.5 to 4 years, respectively. Follow-up data in the 1- to 4-year interval from baseline were available for 48 patients for logMAR and 64 patients for fERG. For each time bin, only one datum per patient was considered (see Methods).

Figure 7A plots the left eye logMAR decay versus the corresponding right eye decay after 1 to 2.5 years from baseline (left) and after 2.5 to 4 years from baseline (right). Figure 7B similarly illustrates the available measures of fERG decline from baseline. Preliminary tests showed high intereye concordance between baseline values in this subset, as well as independence of decline values from baseline (not shown).

The results of the statistical tests assessing the similarity of the fellow eyes in visual function decay over time are shown in Table 3 and reported schematically in Figure 7.

As for baseline data, all tests indicate a high degree of similarity in disease progression between the fellow eyes of CRD patients as measured by logMAR and fERG decay from baseline.

Bilateral Symmetry in ABCA Mutation Carriers

In light of the increasing interest focused on CRDs associated with *ABCA4* gene mutations,[27,28] we studied the degree of bilateral symmetry in the subset of the 61 CRD patients in our cohort who carried likely disease-causing mutations in the *ABCA4* gene.

Among these patients, 56 had bilateral logMAR measurements and 60 had bilateral fERG measurements. Only baseline measurements were available. These data are shown in Figure 8.

The results of the tests assessing the similarity of visual function in the fellow eyes are shown in Table 4 and reported schematically in Figure 8. They indicate a high degree of

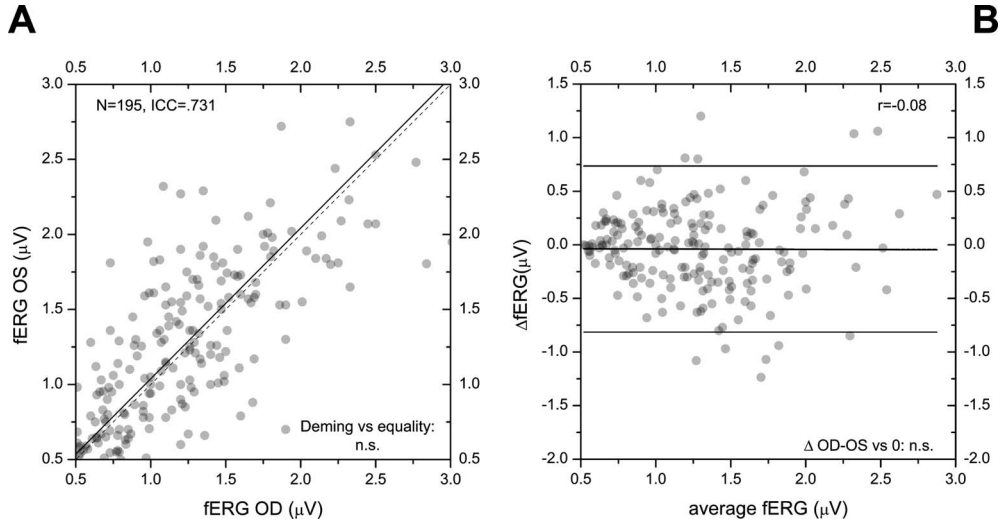

FIGURE 6. Bilateral symmetry in baseline fERG measures in CRD patients above 0.5-μV cutoff. (**A**) Baseline fERG for the left eye plotted against the corresponding right eye fERG for each of the 195 CRD patients with baseline fERG > 0.5 μV (2 decimals) in both eyes. *Symbols* are partially transparent to allow viewing of superimposed data. *Dashed line* is the diagonal, *continuous line* is the Deming regression line. (**B**) Bland-Altman plot for the same data as in (**A**). The mean and mean ± 2 SD lines are indicated. Statistical summary and abbreviations as in Figure 1.

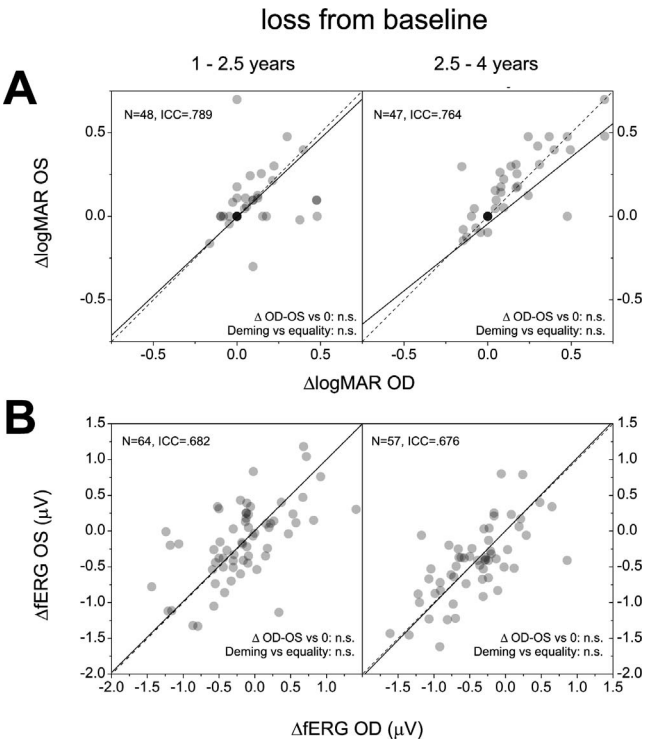

Figure 7. Bilateral symmetry in logMAR and fERG decline from baseline in CRD patients with 4-year follow-up. (**A**) Losses in visual acuity in the right eye plotted against the corresponding variation in visual acuity observed in the left eye between 1 and 2.5 years from baseline (*left*) and in the following 2.5- to 4-year interval. Visual acuity is expressed as logMAR. (**B**) Losses in fERG amplitude in the right eye plotted against the corresponding variation in fERG amplitude observed in the left eye between 1 and 2.5 years from baseline (*left*) and in the following 2.5- to 4-year interval. *Dashed lines* are the diagonal (left = right measure), *continuous lines* are the Deming regression lines. *Symbols* are partially transparent to allow viewing of superimposed data. Statistical summary and abbreviations as in Figure 1.

similarity in visual function loss in the fellow eyes of *ABCA4* CRD patients as revealed by logMAR and fERG measurements.

Rating *ABCA4* mutation in three classes of increasing severity according to Fujinami et al.,[29] these patients comprised 12 (20%) class 1, 32 (53%) class 2, and 16 (27%) class 3 cases. No significant effect of mutation severity on intereye differences was observed in the sample. This analysis may suffer, however, from the limited number of cases included.

Discussion

We analyzed interocular variability in visual acuity, fERG, full-field rod-mediated ERG, and full-field cone-mediated ERG in CRDs, using data from 436 CRD patients. The degree of quantitative similarity between the measurements obtained in the two eyes of each patient was assessed using three different and complementary statistical tests, and results were considered in the context of intereye variability in a cohort of normal control patients.

The statistical tests used addressed whether the mean/median intereye difference differed from zero (paired tests), determined whether intereye data agreed without constant or proportional biases (Deming regression), and quantified the degree of quantitative agreement between the measures obtained in the two eyes (ICC). These tests complemented each other and together provided a more complete view than a single test would have done.[23–25]

Our results show that interocular differences in visual acuity, fERG, and full-field cone- and rod-mediated ERGs in CRD patients are not statistically significant; left and right eye measurements display high values of interclass correlation; and their relationship can be fitted by an equality line. Interocular variability in CRD patients was very similar to that of normal control subjects.

This analysis was prompted by and parallels a similar study performed for retinitis pigmentosa patients.[30] Our results formalize and quantify, on a large patient cohort, the general clinical impression that the loss of visual function is commonly symmetrical in the two eyes of CRD patients.[12,13] This study complements previous observations, based on a limited number of patients, reporting bilateral symmetry of the fellow eyes in CRD fundus appearance,[14–16] visual acuity,[14] and multifocal ERG recordings.[17]

The main novel features of the present study are the high amount of patient data and the use of a set of complementary tests to assess the relatedness of quantitative traits between the fellow eyes for the four clinical indexes considered.

The present analysis has been focused on visual impairments as assessed with functional measures only (visual acuity,

Table 4. Summary of Statistical Tests of Bilateral Symmetry on Baseline Measurements of the *ABCA4* Mutation Carrier

		logMAR			fERG	
ABCA4	***N***	**Mean**	**SD**	***N***	**Mean**	**SD**
OD	56	−0.855	0.496	60	0.504	0.401
OS		−0.809	0.556		0.475	0.437
OD-OS		−0.046	0.408		0.029	0.248
		Paired *t*	**Wilcoxon**		**Paired *t***	**Wilcoxon**
Matched paired tests		0.4	0.267		0.376	0.324
	Estimate	**95%CI low**	**95%CI up**	**Estimate**	**95%CI low**	**95%CI up**
Deming regression						
Intercept	0.196	−0.099	0.491	−0.085	−0.189	0.020
Slope	1.175	0.812	1.538	1.111	0.858	1.364
ICC	0.701	0.539	0.813	0.825	0.724	0.892

Abbreviations as in Tables 1 and 2.

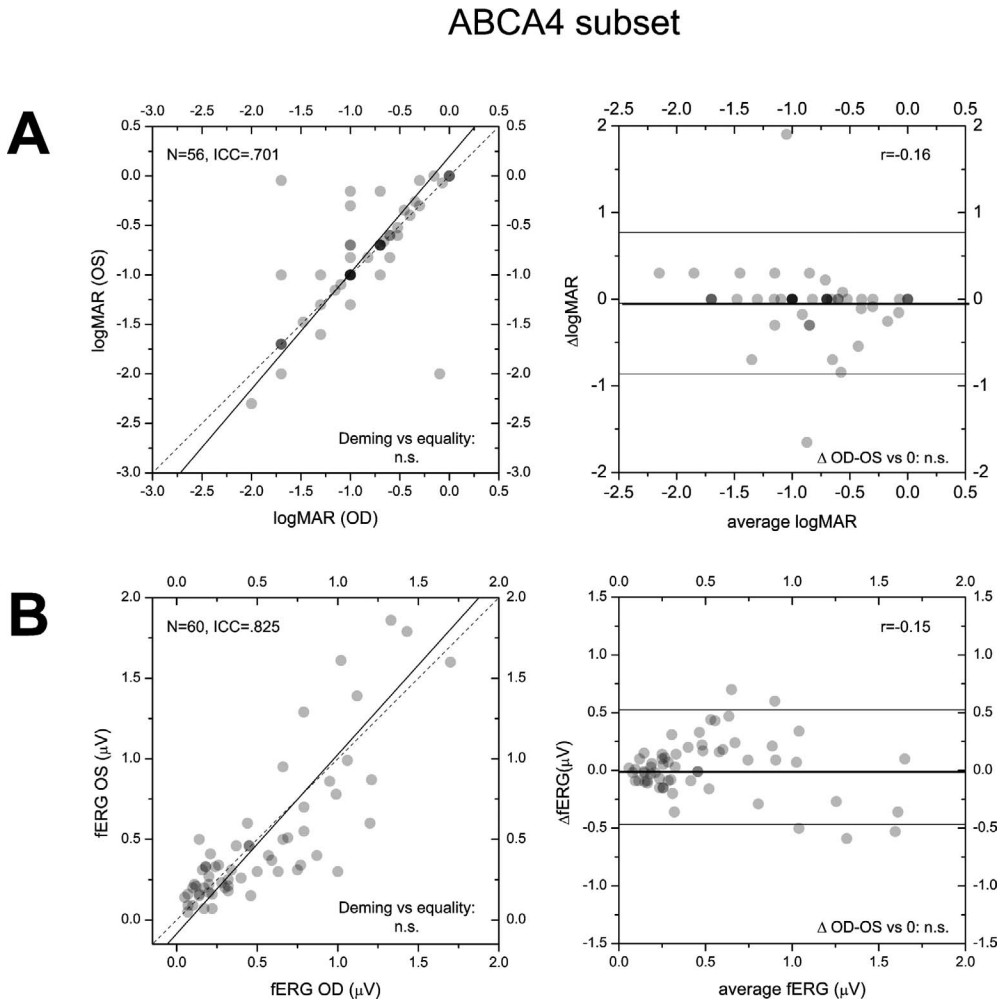

Figure 8. Bilateral symmetry in baseline measures in CRD patients carrying mutations of the *ABCA4* gene. (**A**) Left versus right eye baseline logMAR (*right*) and Bland-Altman plot of the same data for the 56 *ABCA* mutation carriers in the cohort with logMAR measures in both eyes. (**B**) Left versus right eye baseline fERG (*right*) and Bland-Altman plot of the same data for the 60 *ABCA* mutation carriers in the cohort with fERG measures in both eyes. In the *left-hand* plots, the *dasbed lines* are the diagonal, the *continuous lines* the Deming regression lines. In the *right-hand* plots, *horizontal lines* indicate the mean and mean ± 2 SD. *Dots* are partially transparent to allow viewing of superimposed data. Statistical summary and abbreviations as in Figure 1.

fERG, and Ganzfeld cone and rod electroretinograms). A necessary future step will be to understand the degree of bilateral symmetry assessed through quantitative examinations of the retinal structure. This is particularly important considering that while functional analysis can powerfully assess visual function, structural examinations are the elective tools to determine the characteristics and pattern of photoreceptor loss at the basis of the disease.

The finding of a high degree of bilateral symmetry of the fellow eyes in functional visual impairment in CRDs may contribute to a better understanding of the natural course of these pathologies. The present analysis showed that bilateral symmetry characterized both the extent and the rate of functional visual loss in CRD patients. This suggests a high degree of interocular congruence in the pattern and natural history of functional retinal degeneration. Why this should be the case is an open question.

A number of studies report considerable symmetry in the central retinal features of the fellow eyes in normal subjects, including central cone photoreceptor density evaluated with adaptive optics,[31,32] optical coherence tomography measures of macular thickness,[33] macular pigment density,[34,35] and macular blood flow.[36] In light of these data, one could speculate that under the action of common mechanistic noxious determinants (such as genetic mutations, environmental and systemic factors), the likelihood of photoreceptor dysfunction and loss would have a similar retinal distribution in the two eyes of a patient, eventually resulting in bilateral symmetry of functional visual loss.

The high degree of bilateral symmetry in functional visual loss in CRDs seems to support the feasibility of trial designs treating one eye and employing the fellow eye as internal control.

Acknowledgments

Supported by the Programma Nazionale della Ricerca del Consiglio Nazionale delle Ricerche, Aging Program (INVECCHIAMENTO) 2012–2014 to the Istituto di Neuroscienze, Consiglio Nazionale delle Ricerche (LG-R), and Progetto Neuroprotezione, linea D1, Ministero dell'Istruzione e della Ricerca Scientifica (BF). The contribution by Fondazione Bietti in this paper was supported by the Ministry of Health and Fondazione Roma (LZ).

Disclosure: **L. Galli-Resta**, None; **B. Falsini**, None; **G. Rossi**, None; **M. Piccardi**, None; **L. Ziccardi**, None; **A. Fadda**, None; **A. Minnella**, None; **D. Marangoni**, None; **G. Placidi**, None; **F. Campagna**, None; **E. Abed**, None; **M. Bertelli**, None; **M. Zuntini**, None; **G. Resta**, None

References

1. Berson EL, Gouras P, Gunkel RD. Progressive cone-rod degeneration. *Arch Ophthalmol*. 1968;80:68–76.
2. Bird AC. The Duke-Elder Lecture, 1981. Retinal receptor dystrophies. *Trans Ophthalmol Soc U K*. 1981;101:39–47.
3. Ripps H, Noble KG, Greenstein VC, Siegel IM, Carr RE. Progressive cone dystrophy. *Ophthalmology*. 1987;94:1401–1409.
4. Yagasaki K, Jacobson SG. Cone-rod dystrophy. Phenotypic diversity by retinal function testing. *Arch Ophthalmol*. 1989;107:701–708.
5. Michaelides M, Hardcastle AJ, Hunt DM, Moore AT. Progressive cone and cone-rod dystrophies: phenotypes and underlying molecular genetic basis. *Surv Ophthalmol*. 2006;51:232–258.
6. Hamel CP. Cone rod dystrophies. *Orphanet J Rare Dis*. 2007;2:7.
7. Thiadens AA, Phan TM, Zekveld-Vroon RC, et al. Clinical course, genetic etiology, and visual outcome in cone and cone-rod dystrophy. *Ophthalmology*. 2012;119:819–826.
8. Gilbert C, Rahi J, Eckstein M, Foster A. Hereditary disease as a cause of childhood blindness: regional variation. Results of blind school studies undertaken in countries of Latin America, Asia and Africa. *Ophthalmic Genet*. 1995;16:1–10.
9. Bramall AN, Wright AF, Jacobson SG, McInnes RR. The genomic, biochemical, and cellular responses of the retina in inherited photoreceptor degenerations and prospects for the treatment of these disorders. *Annu Rev Neurosci*. 2010;33:441–472.
10. Dalkara D, Sahel JA. Gene therapy for inherited retinal degenerations. *C R Biol*. 2014;337:185–192.
11. Thompson DA, Ali RR, Banin E, et al. Advancing therapeutic strategies for inherited retinal degeneration: recommendations from the Monaciano Symposium. *Invest Ophthalmol Vis Sci*. 2015;56:918–931.
12. Franceschetti A, Francois J, Babel J. *Les hérédo-dégénérescences chorio-rétiniennes (Dégénérescences Tapéto-Rétiniennes)*. Paris: Masson et Cie; 1963.
13. Tasman W, Jaeger E, eds. *Duane's Ophthalmology*. Lippincott Williams & Wilkins; 2013.
14. Fishman GA, Stone EM, Grover S, et al. Variation of clinical expression in patients with Stargardt dystrophy and sequence variations in the ABCR gene. *Arch Ophthalmol*. 1999;117:504–510.
15. Burke TR, Duncker T, Woods RL, et al. Quantitative fundus autofluorescence in recessive Stargardt disease. *Invest Ophthalmol Vis Sci*. 2014;55:2841–2852.
16. Fujinami K, Zernant J, Chana RK, et al. Clinical and molecular characteristics of childhood-onset Stargardt disease. *Ophthalmology*. 2015;122:326–334.
17. Tosha C, Gorin MB, Nusinowitz S. Test-retest reliability and inter-ocular symmetry of multi-focal electroretinography in Stargardt disease. *Curr Eye Res*. 2010;35:63–72.
18. Boye SE, Boye SL, Lewin AS, Hauswirth WW. A comprehensive review of retinal gene therapy. *Mol Ther*. 2013;21:509–519.
19. McCulloch DL, Marmor MF, Brigell MG, et al. ISCEV Standard for full-field clinical electroretinography (2015 update). *Doc Ophthalmol*. 2015;130:1–12.
20. Abed E, Piccardi M, Rizzo D, et al. Functional loss of the inner retina in childhood optic gliomas detected by photopic negative response. *Invest Ophthalmol Vis Sci*. 2015;56:2469–2474.
21. Galli-Resta L, Piccardi M, Ziccardi L, et al. Early detection of central visual function decline in cone-rod dystrophy by the use of macular focal cone electroretinogram. *Invest Ophthalmol Vis Sci*. 2013;54:6560–6569.
22. Berson EL, Rosner B, Weigel-DiFranco C, Dryja TP, Sandberg MA. Disease progression in patients with dominant retinitis pigmentosa and rhodopsin mutations. *Invest Ophthalmol Vis Sci*. 2002;43:3027–3036.
23. Linnet K. Performance of Deming regression analysis in case of misspecified analytical error ratio in method comparison studies. *Clin Chem*. 1998;44:1024–1031.
24. Muller R, Buttner P. A critical discussion of intraclass correlation coefficients. *Stat Med*. 1994;13:2465–2476.
25. Shoukri MM, Pause CA. *Statistical Methods for Health Sciences*. 2nd ed. London: CRC Press; 1999.
26. Chang A. *StatsToDo*. 2015. Available at: http://statstodo.com. Accessed June 29, 2016.
27. Kitiratschky VB, Grau T, Bernd A, et al. ABCA4 gene analysis in patients with autosomal recessive cone and cone rod dystrophies. *Eur J Hum Genet*. 2008;16:812–819.
28. Cideciyan AV, Swider M, Aleman TS, et al. ABCA4 disease progression and a proposed strategy for gene therapy. *Hum Mol Genet*. 2009;18:931–941.
29. Fujinami K, Lois N, Davidson AE, et al. A longitudinal study of stargardt disease: clinical and electrophysiologic assessment, progression, and genotype correlations. *Am J Ophthalmol*. 2013;155:1075–1088, e13.
30. Massof RW, Finkelstein D, Starr SJ, et al. Bilateral symmetry of vision disorders in typical retinitis pigmentosa. *Br J Ophthalmol*. 1979;63:90–96.
31. Lombardo M, Lombardo G, Schiano Lomoriello D, et al. Interocular symmetry of parafoveal photoreceptor cone density distribution. *Retina*. 2013;33:1640–1649.
32. Zhang T, Godara P, Blanco ER, et al. Variability in human cone topography assessed by adaptive optics scanning laser ophthalmoscopy. *Am J Ophthalmol*. 2015;160:290–300, e1.
33. El-Ashry M, Hegde V, James P, Pagliarini S. Analysis of macular thickness in British population using optical coherence tomography (OCT): an emphasis on interocular symmetry. *Curr Eye Res*. 2008;33:693–699.
34. Kanis MJ, Berendschot TT, van Norren D. Interocular agreement in melanin and macular pigment optical density. *Exp Eye Res*. 2007;84:934–938.
35. Raman R, Rajan R, Biswas S, Vaitheeswaran K, Sharma T. Macular pigment optical density in a South Indian population. *Invest Ophthalmol Vis Sci*. 2011;52:7910–7916.
36. Kimura I, Shinoda K, Tanino T, et al. Scanning laser Doppler flowmeter study of retinal blood flow in macular area of healthy volunteers. *Br J Ophthalmol*. 2003;87:1469–1473.

Investigative Ophthalmology & Visual Science